Effect of long-range correlation on the metal-insulator transition in a disordered molecular crystal

Mikael Unge* and Sven Stafström†
Department of Physics, Chemistry and Biology, IFM, Linköpings Universitet, SE-581 83 Linköping, Sweden
(Received 9 August 2006; revised manuscript received 10 October 2006; published 1 December 2006)

Localization lengths of the electronic states in a disordered two-dimensional system, resembling highly anisotropic molecular crystals such as pentacene, have been calculated numerically using the transfer matrix method. The disorder is based on a model with small random fluctuations of induced molecular dipole moments which give rise to long-range correlated disorder in the on-site energies as well as a coupling between the on-site energies and the intermolecular interactions. Our calculations show that molecular crystals such as pentacene can exhibit states with very long localization lengths with a possibility to reach a truly metallic state.

DOI: 10.1103/PhysRevB.74.235403 PACS number(s): 71.30.+h, 71.20.Rv, 71.23.An

I. INTRODUCTION

Molecular crystals as active materials in electronic devices have gained considerable interest during recent years. Pentacene is reported to have the highest field-effect mobility values for organic field-effect transistors (OFETs) and also to have good environmental stability.[1–3] Pentacene OFETs with low (2.5 V) operating voltage have also been demonstrated.[4] This feature increases the possibility to use pentacene OFETs in real applications. However, the charge transport in pentacene molecular crystals is not yet fully understood; in particular, whether or not the observed high mobility can be explained by band transport.

The mean free path of the charge carrier should be significantly larger than the lattice parameter for the band transport model to be valid. An upper limit to the mean free path is the localization length. Hence, molecular crystals of pentacene should have extended states or at least states delocalized over larger regions in order for band transport to occur. The relatively weak interactions in a van der Waals bonded molecular solid, compared to, e.g., a covalent bonded crystal, yield temperature induced disorder due to displacements and rotations of the pentacene molecules. This type of disorder affects both the on-site potential (diagonal disorder) and the intermolecular interaction (off-diagonal disorder).[5]

In studies of systems with diagonal disorder, the Anderson model is widely used.[6] Introduction of random (uncorrelated) disorder in this model results in localized states in one and two dimensions. The pentacene crystal can be considered a two-dimensional system since the intermolecular interactions in the third dimension are very small compared to the two others.[7] Thus, band motion is not possible in the presence of random disorder, which we have previously shown.[8] However, it is well known that long-range correlations in the disorder can yield delocalized states in both one and two dimensions.[9–12] Even short-range correlation in the so called random-dimer model can yield extended states.[13]

It is highly likely that the dominating disorder in molecular crystals is not completely random but contains long-range correlations. The reason is that charges present in solids of large polarizable molecules yield a polarization cloud around the carrier. With structural disorder in the form of displacements and rotations of the individual molecules with respect to the perfect lattice structure, this polarization cloud gives rise to long-range correlated disorder in both the on-site and off-diagonal matrix elements as well as a coupling between on-site and hopping disorder.[5,14] The charge that induces the polarization can be the carrier of the electric current itself, in this case the carrier is dressed by a polarization cloud and referred to as an electronic polaron or Coulomb polaron.[15] Another possible source of this type of disorder is charged impurity ions located in the molecular crystal or in the substrate on which the crystal is grown.[14]

In this paper we use finite size scaling to study the effect of on-site and off-diagonal disorder with long-range correlation on the metal-insulator transition (MIT) in a two-dimensional (2D) system. The results are discussed in the context of pentacene molecular crystals, but can be applied to any 2D system described by a tight-binding model with both on-site and off-diagonal disorder with long-range correlation. We also study the effect on the localization length by the introduction of molecular interaction between next nearest neighbor in addition to nearest neighbor interaction.

II. METHODOLOGY

A two-dimensional rectangular lattice with width N and length M is used as a model for the pentacene molecular crystal (see Fig. 1), and the localization length is calculated numerically, using transfer matrices and Lyapunov exponents.

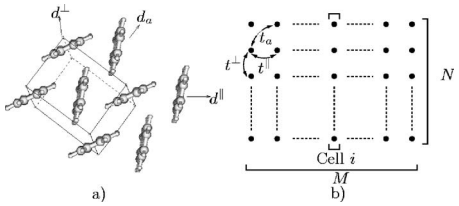

FIG. 1. (a) The pentacene crystal. The triclinic unit cell is indicated by the parallelepiped. The directions $d^{\parallel}$ and $d^{\perp}$ correspond to the directions with the strongest intermolecular interaction. Also, the direction d_a has non-negligible intermolecular interaction. (b) The rectangular lattice, where each point corresponds to a molecule and M and N are the length and width, respectively, of the stripes used in the calculations of the localization lengths.

We use the Hamiltonian derived in Ref. 5,

$$H = \sum_i \varepsilon_i |i\rangle\langle i| - \sum_{i \neq j} t_{ij} \exp\left[\frac{\varepsilon_i + \varepsilon_j}{\delta}\right] |i\rangle\langle j|, \quad (1)$$

where the on-site energies represent the potential due to the induced dipoles, i.e., the polarization cloud discussed above. The off-diagonal terms are the effective transfer integrals corresponding to the bare tight binding parameters scaled (amplified) by disorder due to molecular polarization effects. These effects also introduce a coupling between the on-site and off-diagonal terms in the Hamiltonian. The second summation includes nearest neighbor interactions along the two directions with strongest intermolecular interaction ($d^{\parallel}$ and $d^{\perp}$).[7] The effect of intermolecular interactions in the d_a direction are also studied.

The electronic band considered in this study is the highest molecular orbital (HOMO) of pentacene. Values of the intermolecular transfer integrals of the HOMO orbitals are obtained from Ref. 7 and renormalized according to Ref. 5. The same renormalization constant is used for the three different transfer integrals t_{ij} (see Fig. 1) resulting in the following values: $t^{\parallel}=66$ meV, $t^{\perp}=47$ meV, and $t_a=32$ meV. The strength of the coupling between on-site and off-diagonal elements, δ, is set to 0.4 eV from Ref. 5.

The electric field produced by the fluctuations in the dipole moments will not result in completely random on-site energies. Instead, as discussed above, there is a certain long-range correlation in the potential produced by the variations in this field from site. The correlation function for the on-site energies, ε_i, is $\langle \varepsilon_i(r_i)\varepsilon_j(r_j)\rangle \propto 1/|r_i - r_j|$. The modified Fourier filtering method is used to generate the appropriate correlated on-site energies.[16] A set of numbers $\{u_i\}_{i=1\ldots M\times N}$ with a Gaussian distribution are generated and distributed over a rectangular lattice of size $M \times N$. The mean square of the Gaussian distribution is set to 15.8 meV corresponding to $\pm 3°$ rotation angles of the molecules, which is typical thermal disorder values at room temperature.[5] The two-dimensional Fourier transform of these numbers, $u_{\mathbf{q}}$, is then weighted/filtered by the spectral density, $S(\mathbf{q})$, according to $\varepsilon_{\mathbf{q}} = \sqrt{S(\mathbf{q})} u_{\mathbf{q}}$. The inverse Fourier transform of $\{\varepsilon_{\mathbf{q}}\}$ yields a set of numbers $\{\varepsilon_i\}$ with long-range correlation.

In the modified Fourier filtering method the spectral density is defined as

$$S(\mathbf{q}) = \frac{2\pi}{\Gamma(\beta+1)} \left(\frac{|\mathbf{q}|}{2}\right)^{\beta} K_{\beta}(|\mathbf{q}|), \quad (2)$$

where $\mathbf{q}$ is a vector in reciprocal space, $\beta=(\gamma-2)/2$, K_{β} is the modified Bessel function of the second kind and of order β, and Γ is the gamma function. The strength of the correlation is determined by γ, $\gamma=2(\beta=0)$ corresponds to a very weakly correlated set with contribution from $K_0(|\mathbf{q}|)$ only. The long-range correlation resulting from randomly distributed dipoles correspond to $\gamma=1$.[14]

All calculations presented in this work are performed for this value of γ. It should be noted, however, that deviations from this situation occur if, for instance, the distribution of the rotational angles is somewhat anisotropic as a result of the anisotropy of the crystal structure. In this case, the value of γ would be less than unity. On the other hand, additional screening of the electric field of the induced dipoles leads to a reduction in the correlation and a corresponding increase in the value of γ. The implications of such deviations are discussed in connection to the results presented below.

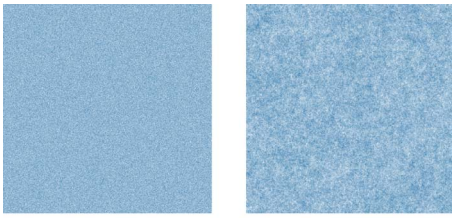

FIG. 2. (Color online) On-site energy plots of square lattices of 1024×1024. (a) Uncorrelated numbers, (b) correlated numbers with $\gamma=1.0$.

Figure 2 shows a set of 1024×1024 correlated uncorrelated (left) and correlated (right) numbers with $\gamma=1.0$. In the uncorrelated set the variations in the numbers are such that they almost average out at the level of resolution of the picture, whereas the correlated set shows much more structure with more or less well-defined regions with close lying on-site energies. The largest set of correlated numbers generated here is $N\times M=512\times 2^{22}\approx 2.1\times 10^9$.

In matrix form the Hamiltonian in Eq. (1) has a block-tridiagonal structure

$$\mathbf{H} = \begin{pmatrix} \mathbf{H}_1 & \mathbf{T}_1 & & & & & \\ \mathbf{T}_1^{\dagger} & \mathbf{H}_2 & \mathbf{T}_2 & & & & 0 \\ & \ddots & \ddots & \ddots & & & \\ & & \mathbf{T}_{i-1}^{\dagger} & \mathbf{H}_i & \mathbf{T}_i & & \\ 0 & & & \mathbf{T}_i^{\dagger} & \mathbf{H}_{i+1} & \mathbf{T}_{i+1} & \\ & & & & \ddots & \ddots & \ddots \end{pmatrix}, \quad (3)$$

where $\mathbf{H}_i$ is a $N\times N$ matrix that describe the on-site and hopping within cell i [see Fig. 1(b)], and $\mathbf{T}_i$ is a $N\times N$ matrix describing the interaction between cell i and cell $i+1$. The secular equation becomes

$$\mathbf{T}_{i-1}^{\dagger}\mathbf{C}_{i-1} + (\mathbf{H}_i - E\mathbf{I})\mathbf{C}_i + \mathbf{T}_i\mathbf{C}_{i+1} = \mathbf{0}, \quad (4)$$

where $\mathbf{C}_i$ is a vector with N coefficients describing the wave function in cell i. From Eq. (4) the transfer matrix is defined as

$$\tau_i(E) = \begin{pmatrix} \mathbf{T}_i^{-1}(E\mathbf{I} - \mathbf{H}_i) & -\mathbf{T}_i^{-1}\mathbf{T}_{i-1}^{\dagger} \\ \mathbf{I} & \mathbf{0} \end{pmatrix}. \quad (5)$$

The transfer matrix gives a connection between the coefficients of the wave function along the system and therefore contains information about the exponential decay of the eigenstates. To determine the localization lengths of the eigenstates we use the concept of Lyapunov exponents, which describe the exponential evolution of the eigenstates.[17] The evolution of the eigenstate is described by the product of the transfer matrices $\tau_i(E)$

$$\mathbf{Q}_M = \prod_{i=1}^{M} \tau_i(E). \tag{6}$$

If the determinant of each $\tau_i(E)$ is nonzero and finite the following matrix exists:[18]

$$\mathbf{\Gamma} = \lim_{M\to\infty} (\mathbf{Q}_M^{\dagger}\mathbf{Q}_M)^{1/2M}. \tag{7}$$

The eigenvalues of Γ is of the type $\exp(\gamma_i)$, where γ_i are the Lyapunov characteristic exponents (LCEs) of $\mathbf{Q}_M$. The LCEs describe the rate of the exponential decay of the eigenstates. The localization length, λ_N, is the inverse of the smallest LCE,[17] which is calculated numerically using an orthogonalization process described by Bettin and Galgani.[19]

The convergence criteria is set to $\Delta\lambda < 0.001$ unit cells. In the calculations with long-range correlation this requires a value of M up to $M=2^{22}$ (see above).

In addition, to study the localization length for the infinite system and to observe a possible MIT we also make use of finite size scaling.[17,20] According to finite size scaling theory[17,20] Λ_N can be expressed as

$$\Lambda_N = f[\xi(w)/N], \tag{8}$$

where $\xi = \lim_{N\to\infty} \lambda_N$. A wave function is localized when the renormalized localization length, Λ_N, decreases with increasing N. A constant or increasing Λ_N with increasing N indicates extended states.[17] By fitting the calculated renormalized localization length to $\Lambda_N = \xi/N + b(\xi/N)^2$ for small Λ_N, it is also possible to obtain the localization length for the infinite system. However, in all cases studied here that include long-range correlations in the disorder, the localization lengths are very long and consequently the value of N has to be even larger to allow for this kind of fitting procedure. Since the computations become very extensive for large values of N, this limits the application of this procedure. The maximum value that we have been able to treat is $N=512$. We therefore use finite size scaling as an indicator of extended states and a possible MIT and not to calculate localization lengths for the infinite systems.

III. RESULTS

First, we study the effect of including the intermolecular interaction, t_a, in the d_a direction. These studies were performed on systems without long-range correlations in the disorder and with the coupling between on-site and off-diagonal elements excluded. The off-diagonal elements are in this case generated from Eq. (1), but using an auxiliary set on-site energies which is completely independent from the energies used in the on-site matrix element.

The results from a set of calculations with N in the range from 8 to 128 are shown in the left panels in Fig. 3. In the lower left panel the intermolecular t_a interaction is absent which results in moderate localization lengths, ~16 unit cells for the largest system. The introduction of t_a (top left panel) yields an increase in λ_N with a factor of ~1.4 and a shift of the maximum localization lengths to negative energies.

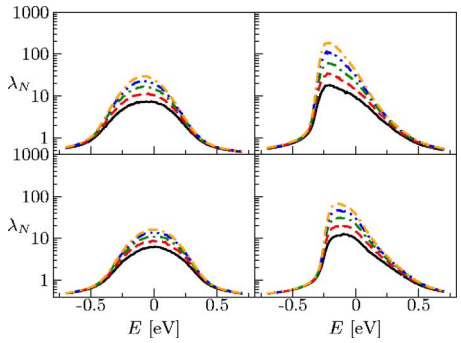

FIG. 3. (Color online) Localization length, λ_N, vs energy, E, for different N; 8 (lowest curve in each panel), 16, 32, 64, and 128 (uppermost curve). The two left and the two right panels correspond to uncorrelated disorder and uncorrelated disorder with coupling between the on-site and off-diagonal terms, respectively. The upper and lower panels are results with and without t_a included, respectively.

In the right panels in Fig. 3 are shown the result including the coupling between the on-site and off-diagonal matrix elements. These results are still with the long-range correlations excluded. The localization lengths increase quite dramatically compared to the system discussed above with λ_N reaching close to 68 lattice units in the case with t_a excluded (lower right panel) and above 185 lattice units with t_a included. Note that the mean values and standard deviation of the distribution of both on-site and off-diagonal matrix elements are the same with and without coupling included. Thus, the increase in the localization length is due to the qualitative difference between the two distributions. This difference also results in a shift in the maximum of λ_N towards negative energies by ~0.2 eV in the right panels (with coupling between on-site and off diagonal matrix elements) compared to the left panels. To some extent this shift is also present in the density of states (DOS) which we have calculated for a finite system of size 64×150. The DOS plots are shown in Fig. 4 for the four different types of systems discussed above. The difference in shape in the DOS can be explained by the fact that the largest values of the intermo-

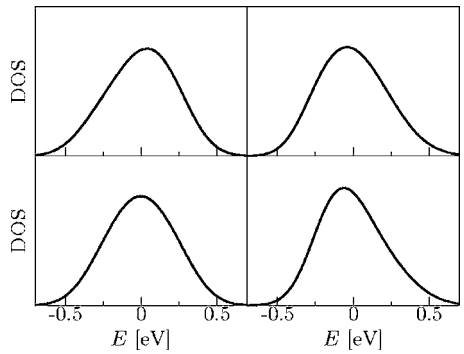

FIG. 4. Density of states, DOS (arb. units), vs energy, E, for system of size 64×150. The two left and the two right panels correspond to uncorrelated disorder and uncorrelated disorder with coupling between the on-site and off-diagonal terms, respectively. The upper and lower panels are results with and without t_a included, respectively.

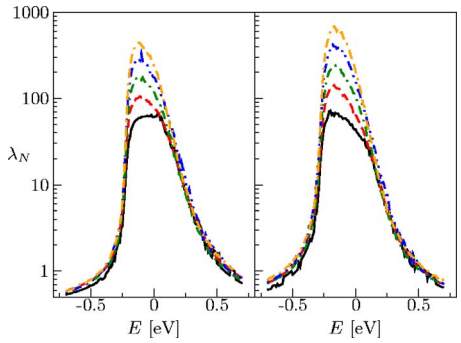

FIG. 5. (Color online) Localization length, λ_N, vs energy, E, with long-range correlation, $\gamma=1.0$ for different N; 8, 16, 32, 64 and 128. The right plot include t_a.

lecular interaction strength occur between sites with positive on-site energies [see Eq. (1)]. The bonding linear combination of atomic orbitals (LCAO) form eigenstates at energies slightly below $\varepsilon=0$. States with large bonding LCAO contributions on these strongly coupled sites are also the most extended states observed in Fig. 3. Since the coupling between large positive energies and large intermolecular interaction strengths is missing in the uncoupled model, the localization lengths become shorter in this case.

We now proceed by introducing long-range correlations into the on-site energies. The result for these calculations are shown in Fig. 5 without (left panel) and with (right panel) intermolecular interaction in the d_a direction included. The coupling between the on-site and off-diagonal terms is included in both graphs, hence the intermolecular interaction term includes long-range correlation. In these systems, the localization length reaches ~446 unit cells and ~683 unit cells without and with t_a, respectively. Thus, the localization length increases by a factor of 4–5 compared to the case with uncorrelated disorder. This is purely an effect of the long-range correlation since the mean values and standard deviation of the distribution of both on-site and off-diagonal matrix elements are the same in both cases. The maximum values of λ_N are shifted towards negative energies for the same reason as discussed above.

It is clear from Fig. 5 that the localization lengths of the states in the band tails are much shorter than in the center of the band. Furthermore, these localization lengths do not scale with the width of the system but remain approximately constant for increasing N. This is a clear indication that the region of the band tails contain localized states and with the Fermi level positioned in this region, the system should behave as an insulator. Note however, that the DOS is small in these regions and even moderate (field effect) charging of the molecular layer can shift the Fermi energy into the region where the localization lengths scale with N.

We now turn to investigate the scaling properties of the localization length. Λ_N is calculated as a function of N for both systems presented in Fig. 5 as well as for three of the four systems presented in Fig. 3 (the case with no coupling and t_a is excluded). Due to the different energies at which the peak in the localization length occur, we choose to study the scaling behavior at energies corresponding to the maximum localization length in the spectra shown in Figs. 3 and 5.

TABLE I. Energies used in the finite size scaling analysis corresponding to the maximum localization lengths for the different models.

Model	$E_{\max\lambda}$ (eV)
Uncorr.	0.00
Coupling	−0.13
Coupling with t_a	−0.22
Long-range corr.	−0.12
Long-range corr. with t_a	−0.17

These energies are listed in Table I. The results are shown in Fig. 6 for N up to 256 in all cases and also for $N=512$ for the two cases of correlated disorder, i.e., the cases with the largest values of λ_N.

Clearly there is a large difference between the results of the systems with long-range correlation presented in Fig. 6 and those of the uncorrelated model. The uncorrelated system yields localization lengths for the two-dimensional system of 17 unit cells at $N=256$, corresponding to 7 nm, assuming an intermolecular distance of 4 Å. With long-range correlations included, the localization length reaches 678 unit cells without t_a included and 1074 unit cells with t_a included. The finite-size scaling results up to $N=256$ still show a localized behavior, i.e., Λ_N is decreasing with increasing N. Since the systems with the most extended wave functions could be close to a MIT, we have performed calculations with $N=512$ for these cases in order to look for a possible change in the behavior of Λ_N. The maximum localization length obtained is 2115 unit cells, which corresponds to 0.85 μm. Compared to the system with uncorrelated disorder and no coupling between the diagonal and off-diagonal disorder, this is an increase of the localization length by more than two orders of magnitude.

The renormalized localization lengths for the system with t_a included show a tendency to saturate at a value of $\Lambda_N \sim 4$ (topmost curve in the lower panel in Fig. 6). According to finite size scaling this indicates that the system is reaching the transition from an insulating to a metallic state.[17] Unfor-

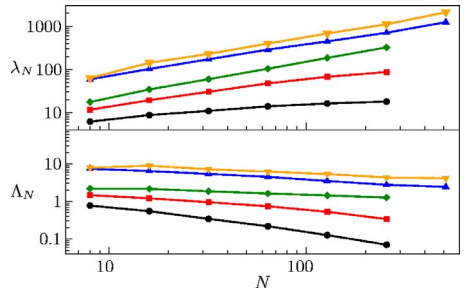

FIG. 6. (Color online) Localization length, λ_N, and renormalized localization length, Λ_N, vs N. Uncorrelated (circles), coupling between the on-site and off-diagonal terms (squares), coupling between the on-site and off-diagonal terms with t_a (diamonds), long-range correlation $\gamma=1.0$ without (triangle up) and with (triangle down) t_a. The solid lines are a guide to the eye. The localization lengths are calculated at the energies specified in Table I. The deviation for each calculated value are within the size of the symbols.

tunately, at present we are unable to perform calculations for even larger values of N to give a more conclusive result concerning the MIT. Note that the particular type and strength of the disorder used in our calculations represent the behavior of a typical molecular crystal such as pentacene. It is of course possible to drive the model system further towards the metallic state by increasing the correlation factor below the present value of $\gamma=1$ (or alternatively, reduce the width of the Gaussian distribution of on-site energies or increase the intermolecular interaction strength). This would, however, require another type of correlated disorder than that obtained from the random dipole model. It will be the subject of further studies to include conductivity in the model and to relate the results obtained here to the experimental result of bandlike transport of single crystals of pentacene at room temperature.[3]

IV. CONCLUSIONS

In conclusion, the results presented here show that molecular crystals such as pentacene can exhibit extended states only if there exists correlation in the static disorder. The existence of this type of disorder is motivated by the model of randomly oriented induced dipole moments. Our results show a substantial increase in the localization length of the electronic state with correlated disordered as compared to the case of uncorrelated disorder. The localization length exceeds the lattice constant by more than three orders of magnitudes when calculated for a stripe of the molecular crystal with a width of 512 lattice sites. The renormalized localization length indicates a transition into an extended state which can explain the experimental observation of bandlike transport of single crystals of pentacene at room temperature.[3]

ACKNOWLEDGMENTS

Financial support from the Swedish Research Council (V.R.) is gratefully acknowledged. We also thank the National Supercomputer Centre in Linköping for providing code development support and computational facilities.

*Electronic address: mikun@ifm.liu.se
†Electronic address: sst@ifm.liu.se

[1] Y.-Y. Lin, D. J. Gundlach, S. F. Nelson, and T. N. Jackson, IEEE Electron Device Lett. **18**, 606 (1997).
[2] C. D. Dimitrakopoulos, S. Purushothaman, J. Kymissis, A. Callegari, and J. M. Shaw, Science **283**, 822 (1999).
[3] O. D. Jurchescu, J. Baas, and T. T. M. Palstra, Appl. Phys. Lett. **84**, 3061 (2004).
[4] M. Halik, H. Klauk, U. Zschieschang, G. Schmid, C. Dehm, M. Schütz, S. Maisch, F. Effenberger, M. Brunnbauer, and F. Stellacci, Nature (London) **43**, 963 (2004).
[5] M. N. Bussac, J. D. Picon, and L. Zuppiroli, Europhys. Lett. **66**, 392 (2004).
[6] P. W. Anderson, Phys. Rev. **109**, 1492 (1958).
[7] Y. C. Cheng, R. J. Silbey, D. A. da Silva Filho, J. P. Calbert, J. Cornil, and J. L. Brédas, J. Chem. Phys. **118**, 3764 (2003).
[8] M. Unge and S. Stafström, Synth. Met. **139**, 239 (2003).
[9] F. A. B. F. de Moura and M. L. Lyra, Phys. Rev. Lett. **81**, 3735 (1998).
[10] W.-S. Liu, S. Y. Liu, and X. L. Lei, Eur. Phys. J. B **33**, 293 (2003).
[11] S.-J. Xiong and G.-P. Zhang, Phys. Rev. B **68**, 174201 (2003).
[12] H. Shima, T. Nomura, and T. Nakayama, Phys. Rev. B **70**, 075116 (2004).
[13] D. H. Dunlap, H.-L. Wu, and P. W. Phillips, Phys. Rev. Lett. **65**, 88 (1990).
[14] V. V. Flambaum and V. V. Sokolov, Phys. Rev. B **60**, 4529 (1999).
[15] Y. Toyozowa, Prog. Theor. Phys. **12**, 421 (1954).
[16] H. A. Makse, S. Havlin, M. Schwartz, and H. E. Stanley, Phys. Rev. E **53**, 5445 (1996).
[17] J. L. Pichard and G. Sarma, J. Phys. C **14**, 127 (1981).
[18] V. I. Oseledec, Trans. Mosc. Math. Soc. **19**, 197 (1968).
[19] G. Benettin and L. Galgani, in *Intrinsic Stochasticity in Plasmas*, edited by G. Laval and D. Grésillon (Editions de Physique, Orsay, 1979), p. 93.
[20] A. MacKinnon and B. Kramer, Phys. Rev. Lett. **47**, 1546 (1981).